

Intracavity wavelength modulation of an optical parametric oscillator for coherent Raman microscopy

Brian G. Saar^{1,†}, Gary R. Holtom^{1,†}, Christian W. Freudiger^{1,2}, Chrisita Ackermann³, Winfield Hill⁴ and X. Sunney Xie^{1,*}

¹Department of Chemistry and Chemical Biology, Harvard University, Cambridge, MA 02138, USA

²Department of Physics, Harvard University, Cambridge, MA 02138, USA

³Ackermann Associates, 203 W. Michigan Av., Saline, MI 48176, USA

⁴The Rowland Institute at Harvard, Harvard University, Cambridge, MA 02142, USA

[†]equal contributors

*xie@chemistry.harvard.edu

Abstract: We present a novel intracavity frequency modulation scheme in a tunable, picosecond optical parametric oscillator (OPO). The OPO signal wavelength can be modulated with a depth of more than 10 nm at a rate of 38 MHz (one half its repetition rate). We discuss the design and construction of the light source and its application to the recently-developed frequency modulation coherent anti-Stokes Raman scattering (FM-CARS) and stimulated Raman scattering (SRS) techniques. The new light source allows for real time subtraction of the interfering background signal in coherent Raman imaging, yielding images with purely chemical contrast.

©2009 Optical Society of America

OCIS codes: (190.4360) Nonlinear optics, devices; (140.3518) Lasers, frequency modulated; (180.4315) Nonlinear microscopy

References and links

1. G. C. Bjorklund, "Frequency-modulation spectroscopy: a new method for measuring weak absorptions and dispersions," *Opt. Lett.* **5**(1), 15 (1980).
2. B. Levine, C. Shank, and J. Heritage, "Surface vibrational spectroscopy using stimulated Raman scattering," *IEEE J. Quantum Electron.* **15**(12), 1418–1432 (1979).
3. M. D. Levenson, W. E. Moerner, and D. E. Horne, "FM spectroscopy detection of stimulated Raman gain," *Opt. Lett.* **8**(2), 108–110 (1983).
4. W. E. Moerner, and L. Kador, "Optical detection and spectroscopy of single molecules in a solid," *Phys. Rev. Lett.* **62**(21), 2535–2538 (1989).
5. C. L. Evans, and X. S. Xie, "Coherent Anti-Stokes Raman Scattering Microscopy: Chemical Imaging for Biology and Medicine," *Annu. Rev. Anal. Chem.* **1**(1), 883–909 (2008).
6. C. W. Freudiger, W. Min, B. G. Saar, S. Lu, G. R. Holtom, C. He, J. C. Tsai, J. X. Kang, and X. S. Xie, "Label-free biomedical imaging with high sensitivity by stimulated Raman scattering microscopy," *Science* **322**(5909), 1857–1861 (2008).
7. F. Ganikhanov, C. L. Evans, B. G. Saar, and X. S. Xie, "High-sensitivity vibrational imaging with frequency modulation coherent anti-Stokes Raman scattering (FM CARS) microscopy," *Opt. Lett.* **31**(12), 1872–1874 (2006).
8. M. C. Fischer, H. Liu, I. R. Piletic, T. Ye, R. Yasuda, and W. S. Warren, "Self-phase modulation and two-photon absorption imaging of cells and active neurons," *Proc. SPIE* **6442**, 64421J (2007).
9. D. J. Jones, E. O. Potma, J.-X. Cheng, B. Burfeindt, Y. Pang, J. Ye, and X. S. Xie, "Synchronization of two passively mode-locked, picosecond lasers within 20 fs for coherent anti-Stokes Raman scattering microscopy," *Rev. Sci. Instrum.* **73**(8), 2843–2848 (2002).
10. W. Demtröder, *Laser Spectroscopy*, 3rd ed. (Springer-Verlag, New York, 2003).
11. C. L. Tang, and J. M. Telle, "Laser modulation spectroscopy of solids," *J. Appl. Phys.* **45**(10), 4503–4505 (1974).
12. J. M. Telle, and C. L. Tang, "New method for electro-optical tuning of tunable lasers," *Appl. Phys. Lett.* **24**(2), 85–87 (1974).
13. L. Cabaret, P. Camus, R. Leroux, and J. Philip, "Intracavity LiNbO₃ Fabry-Perot etalon for frequency stabilization and tuning of a single-mode quasi-continuous-wave titanium:sapphire ring laser," *Opt. Lett.* **26**(13), 983–985 (2001).

14. H. F. Gleeson, A. J. Murray, E. Fraser, and A. Zoro, "An electrically addressed liquid crystal filter for tunable lasers," *Opt. Commun.* **212**(1-3), 165–168 (2002).
 15. A. Godard, and E. Rosencher, "Energy yield of pulsed optical parametric oscillators: a rate-equation analysis," *IEEE J. Quantum Electron.* **40**(6), 784–790 (2004).
 16. X. S. Xie, J. Yu, and W. Y. Yang, "Living cells as test tubes," *Science* **312**(5771), 228–230 (2006).
-

1. Introduction

Frequency modulation (FM) spectroscopy is a well-established method for making sensitive spectroscopic measurements of molecules in the presence of a nonspecific, interfering background signal [1]. In this approach, the excitation wavelength is modulated at high frequency (often MHz) and phase sensitive detection at the modulation frequency of the excitation light is used to distinguish the wavelength-dependent signal of interest from the wavelength-independent background signal. FM spectroscopy using high frequency modulation has allowed exquisite sensitivity in stimulated Raman scattering [2,3] and absorption [4] as early as the 1970s, and numerous variations on the basic theme of real-time background subtraction via high frequency modulation have been implemented.

Over the past decade, coherent Raman microscopy (CRM) techniques based on coherent anti-Stokes Raman scattering (CARS) or stimulated Raman scattering (SRS) have emerged as powerful biomedical imaging modalities that allow label-free imaging based on the intrinsic vibrational signatures of molecules in the sample. In CRM techniques [5,6], pulsed laser beams of two frequencies, called the pump, ω_p , and Stokes, ω_s , are overlapped in space and time and focused onto the sample by a laser-scanning microscope. Chemically-selective imaging is performed when the difference frequency $\omega_p - \omega_s$ matches a vibrational frequency of molecules in the sample. CRM techniques are valuable because they offer chemical contrast with orders of magnitude higher signal level than conventional spontaneous Raman scattering.

In CARS microscopy, emission at the anti-Stokes frequency, $\omega_{as} = 2\omega_p - \omega_s$, is detected, which results from a four-wave-mixing process in the sample. When $\omega_p - \omega_s$ is tuned into resonance with a molecular vibrational transition intrinsic to the sample, the emission at ω_{as} is resonantly enhanced. However, for samples with a weak Raman resonance and/or only a low concentration of the chemical species of interest, CARS suffers from a nonresonant four-wave-mixing background, which can limit the sensitivity of the measurements. This background can be eliminated by rapidly tuning $\omega_p - \omega_s$ rapidly on and off resonance with the Raman-active transition and performing a differential measurement, a technique known as FM-CARS [7].

In SRS microscopy, energy transfer from the pump to the Stokes beam in the presence of a vibrational resonance in the sample is detected by measuring either the loss of energy at ω_p or gain of energy at ω_s . The nonresonant four-wave-mixing background that plagues CARS is eliminated in SRS, yielding high sensitivity. However, SRS microscopy can also suffer from a background due to cross-phase-modulation, thermal lensing or two-color two-photon absorption [8]. By means of proper design of the collection optics and choice of the pump and Stokes wavelengths, the SRS background can be made orders of magnitude lower than the background in CARS, making SRS more sensitive [6]. Alternatively, this spurious background can also be eliminated completely by employing frequency modulation. However, until now, an optimized light source for frequency modulation CRM techniques has not been available because of the unique requirements for CRM light sources.

Rapid CRM imaging is ideally performed with a broadly tunable, two color, picosecond light source with high (>10 MHz) repetition rate [5]. In addition, for FM techniques, the modulation frequency must be high (ideally >1 MHz) for two reasons (1) images are formed by rapidly scanning the laser spot across the sample with short pixel dwell times, necessitating rapid tuning of the source at each pixel and (2) laser noise exists predominantly at low frequencies and thus is most efficiently suppressed by modulating at high frequency [2]. In our previous FM-CARS work, no method existed for modulating the wavelength of such a picosecond light source at high frequency, so we made use of a laser system consisting of two

independent ultrafast oscillators with electronic synchronization [9] as well as a synchronously-pumped OPO, which was expensive, complex, difficult to align, and had the possibility of noise sources not common to all laser beams [7].

2. OPO Design and Construction

Here, we report a tunable, picosecond laser system based on a novel, intracavity modulation scheme in an OPO. Previously, intracavity tuning of CW or quasi-CW lasers [10] via electro-optic modulators [11,12], Fabry-Perot etalons [13] or liquid crystal devices [14] has been reported. However, none of those laser sources was appropriate for CRM, and to our knowledge rapid (>1 MHz) modulation of an OPO has not been reported before. Our system provides two synchronized laser beams, one fixed at 1064 nm from an ultrafast oscillator (picoTrain, High Q Laser) which can be used as the Stokes beam, and the other from a synchronously-pumped OPO signal wave tunable from about 750 nm up to 1010 nm which

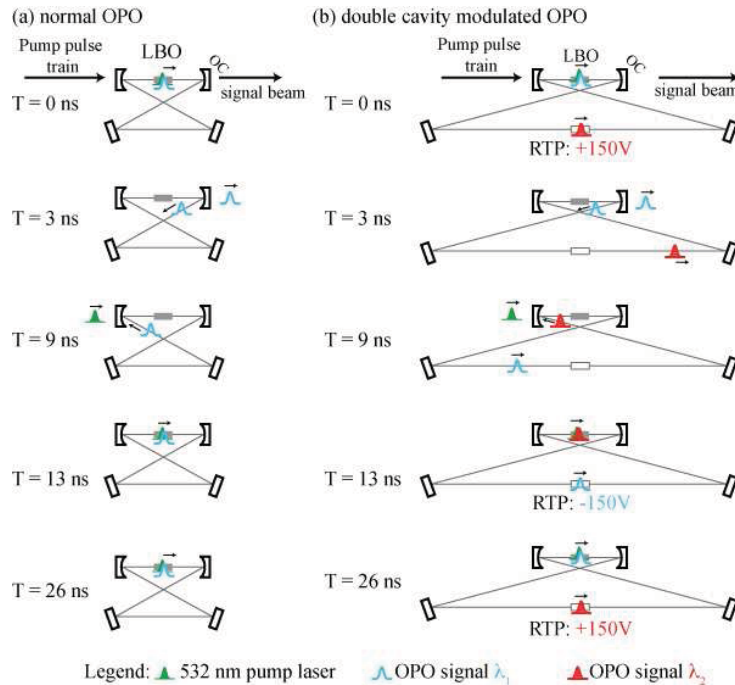


Fig. 1. Operating principle of a normal and double cavity modulated OPO. (a) Operating principle of a representative synchronously-pumped OPO. The round trip time of a pulse in the OPO cavity is exactly matched to the period of the pump laser repetition rate (13 ns). Thus a pulse in the cavity makes exactly one round trip before meeting the next pump laser pulse in the nonlinear LBO crystal, leading to efficient wavelength conversion. Each time a pulse strikes the output coupler (OC), ~ 10 - 20% of the energy exits the cavity and is used for the experiment. (b) Operating principle of the intracavity modulated OPO. Initially ($T = 0$ ns), a pulse of wavelength λ_1 and a pump laser pulse are in the LBO nonlinear crystal gain medium. At the same time, a pulse of λ_2 is in the modulator crystal and the modulation drive waveform which is synchronized to the pulse train reaches its maximum positive value, causing a red shift. Because the OPO has a cavity round trip time equal to *twice* the period of the pump laser repetition rate, at one period of the pump laser repetition rate later ($T = 13$ ns), λ_1 and λ_2 have switched positions so that λ_2 is in LBO crystal while λ_1 is in the modulator crystal. At that time, the drive voltage reaches its maximum negative value, corresponding to a blue-shift. At $T = 26$ ns, the system is returned to the initial, $T = 0$ ns state and the cycle begins again. In this way, the output of the intracavity-modulated OPO consists of alternating pulses of two colors, λ_1 and λ_2 , each at 38 MHz, for a total repetition rate (considering both colors) equal to the 76 MHz pump laser repetition rate.

can be used as the pump beam. The lithium triborate (LBO) crystal ($\theta = 90^\circ$, $\phi = 0^\circ$, $3 \times 3 \times 20$ mm) used is pumped by 532 nm light taken from the frequency-doubled oscillator output, and has a phase matching bandwidth of about 15 nm at constant temperature. A Lyot filter is used to narrow the output bandwidth to 0.3 nm, providing stable operation and fine tuning via rotation of the plates. An electrically tunable Lyot filter might allow the OPO wavelength to be modulated for FM-CARS within the fixed phase-matching bandwidth, eliminating the need to change the LBO crystal temperature, which is a slow process.

Such an electrically tunable Lyot filter was constructed using three optical elements: a static, multi-order quartz waveplate (United Crystal Company), a custom Pockel's cell consisting of two rubidium titanyl phosphate (RTP) crystals at a 140 micron beam waist in the cavity (Raicol Crystals), and a Glan-Brewster prism (MGLBAS5, Karl Lambrecht), which act together to determine the wavelength of minimum loss in the optical cavity. This wavelength can then be modulated by the voltage applied to the Pockel's cell.

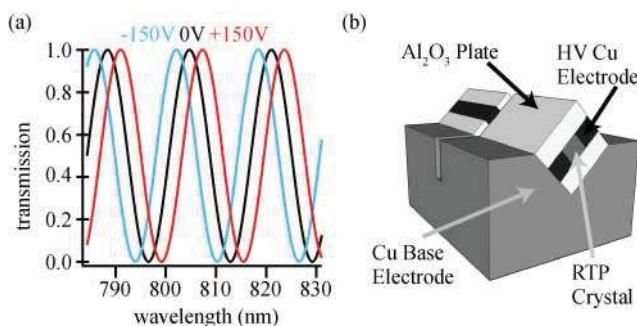


Fig. 2. (a) Schematic modulator transmission versus wavelength for three applied voltages, calculated using the 50λ plate at 800 nm and the 2-mm-thick modulator crystals. (b) Modulator layout, showing thin RTP crystals with perpendicular orientation, sapphire (Al_2O_3) plates to minimize thermal gradients, and the copper (Cu) ground and high voltage (HV) electrodes.

However, even though tuning can be accomplished electrically without changing the LBO temperature, a second challenge must be overcome to implement the necessary high frequency modulation. In a typical synchronously pumped OPO, the pump laser and the OPO have identical cavity lengths so that pulses which travel a round trip inside the cavity meet the next pump laser pulse in the nonlinear crystal (Fig. 1a). OPOs require a large number of such round trips to build up to steady-state operation [15]. Cavity dynamics intrinsic to the OPO thus limit the maximum timescale at which it can be modulated with an intracavity element to much less than 1 MHz, which is too slow for FM-CARS experiments.

To circumvent this problem, we designed an OPO with a cavity length that is exactly twice that of the pump laser source. By doubling the cavity length of our OPO, two completely independent pulse trains can exist simultaneously in the OPO cavity (Fig. 1b). These pulse trains share all optical elements such as the gain medium and mirror set, avoiding differences in the optical path. However, while one pulse is being amplified in the LBO crystal, the other is passing through the custom electro-optic modulator that accomplishes wavelength fine tuning (Fig. 2a). At one period of the pump laser repetition rate later in time, the roles are reversed, so that the two colors alternate in passing through the gain medium and the modulator crystal.

Our pump laser has a repetition rate of 76 MHz, and thus a cavity length of approximately 3.94 m. The OPO then has a cavity length of 7.88 m. The cavity was designed with a focal spot of $80 \mu\text{m}$ in the 2-cm-long LBO gain medium. A custom broadband ($>99.9\%$ reflectivity from 750 to 1100 nm) mirror set was employed (Layertec), with an 85% reflector as the output coupler and a number of flat mirrors to fold the cavity onto a 100×30 cm baseplate. The output polarization was horizontal, matching the 1064 nm light from the pump laser

oscillator, and the output power was greater than 750 mW in the signal wave with 3.5 W of 532 nm pump power.

This sinusoidal voltage that is applied to the modulator was derived from the pump laser repetition rate, and divided by two in frequency, to create a 38 MHz sine wave. We used a continuously variable phase shifter circuit to match the timing of the maximum and minimum voltages of the sine wave to the time when the OPO signal pulses passed through the modulator. The phase-shifted output was amplified using a commercial wideband amplifier (Empower RF Systems), whose output was impedance-matched and then used to drive a resonant “tank” circuit consisting of an air-core inductor and the self-capacitance of the electro-optic crystal. RTP was selected for the tuning element because it combines high nonlinearity and high transparency, allowing for a compact element, and is not hygroscopic. Minimizing thermal gradients ensures stable operation. To do this, we utilized a thin pair of crystals (2x2 mm), each 10 mm in length. The use of two RTP crystals whose principal axes are perpendicular minimizes the static birefringence in the modulator. The two crystals were installed on a large copper base which serves as both a heat sink and the ground electrode. A copper high voltage electrode was placed on top of each crystal (Fig. 2b). The crystals are electrically in parallel and optically in series (i.e. their retardance adds).

By synchronizing the drive voltage to the laser pulse train at one half its fundamental frequency, one pulse train always sees maximum voltage while the other pulse train always sees the minimum. Thus the modulation depth is proportional to the peak-to-peak AC voltage and can be continuously adjusted. We found the $\frac{1}{4}$ wave voltage to be approximately 300 V p-p at 800 nm. At this voltage, a splitting between the two operating wavelengths of about 11 nm ($\sim 140 \text{ cm}^{-1}$ at 870 nm) was observed (Fig. 3a), which is more than sufficient to tune into and out of a typical Raman line. The temporal width of the pulses from the OPO was measured to be 5.7 ps. To confirm the wavelength switching, we separated the two output wavelengths using a diffraction grating (Fig. 3b) and detected each wavelength individually using a high bandwidth photodiode (Fig. 3c).

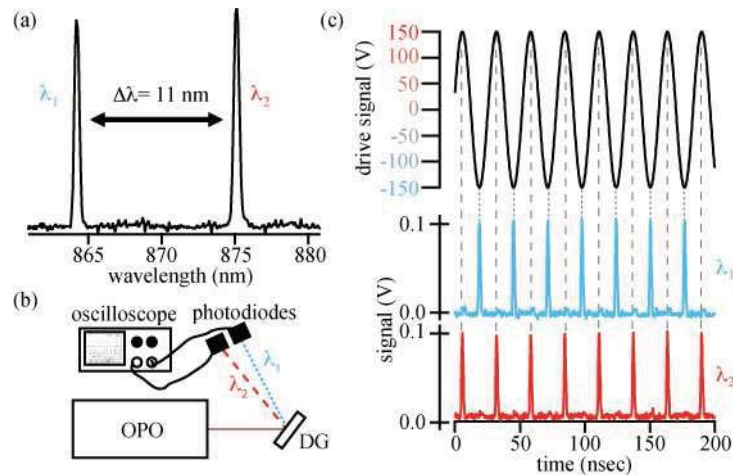


Fig. 3. 38 MHz wavelength switching (a) Optical spectrum of the single beam OPO signal wave, showing 11 nm splitting between the two wavelengths (b) Test setup for verification of the switching behavior. The two wavelengths which comprise the OPO signal beam are separated using a diffraction grating (DG) (600 lines/mm, Edmund Industrial Optics) and simultaneously detected by high speed photodiodes (DET210, Thorlabs). The photodiode output is detected by a high bandwidth oscilloscope (TDS3054b, Tektronix). (c) Top: drive waveform applied to the modulator in the OPO, which causes the 38 MHz switching behavior. Bottom: Simultaneous output of the two high bandwidth photodiodes, each detecting one of the two wavelengths from (a). The dashed lines indicate that the peak voltage of the drive waveform corresponds to λ_2 , while the trough corresponds to λ_1 .

3. Coherent Raman Imaging

The OPO can be used to perform chemically selective CRM imaging by combining the output with the 1064 nm fundamental output of the pump laser to provide pump and Stokes beams, respectively. The combined beams are routed through a laser scanning microscope (Olympus FV300/IX71) and focused onto the sample. For CARS, the emission from the sample is collected by a forward condenser, the anti-Stokes beam is isolated with a shortpass filter (ET750sp-2p8, Chroma Technology) and detected with a photomultiplier tube (PMT) module (H7422-50, Hamamatsu). The output of the PMT is preamplified (C6438-01, Hamamatsu) and detected with a lock-in amplifier (SR844, Stanford Research Systems) that is referenced to the 38 MHz modulator drive waveform.

To verify the chemical selectivity of the technique, we generated deuterated bacterial cells by growing a culture of *M. smegmatis* on deuterated carbon sources and $^2\text{H}_2\text{O}$. By incorporating deuterium into the bacterial cell walls, we were able to use the chemical selectivity of the $\text{C}-^2\text{H}$ stretching band at 2100 cm^{-1} , which is a minimally perturbative vibrational labeling scheme [16]. Deuterated bacteria show high contrast (Fig. 4a) in the FM-CARS image when the on resonance pump is tuned into the $\text{C}-^2\text{H}$ stretching resonance at 2100 cm^{-1} , while the off-resonance wavelength is tuned to 2000 cm^{-1} . In contrast, cells of the same strain that have been grown on ordinary C-H media do not appear in the image (Fig. 4b), despite the fact that a number of cells are present in the simultaneous bright field image (Fig. 4c).

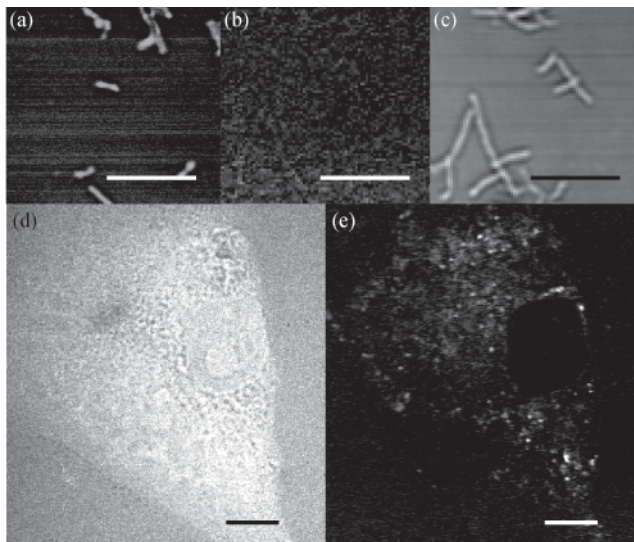


Fig. 4. CARS images using the OPO. (a) FM-CARS image of individual bacterial cells grown on deuterated carbon sources and water, imaged at the $\text{C}-^2\text{H}$ stretching frequency at 2100 cm^{-1} . The off resonance pump wavelength was set at 2000 cm^{-1} . (b) FM-CARS images of bacterial cells imaged under the same conditions but without the deuterated nutrient supply show no contrast. (c) A simultaneous bright field image acquired along with (b) demonstrates that cells are present but do not appear in FM-CARS unless they are deuterated. (d) Normal CARS image of a mammalian cell incubated with deuterated oleic acid, acquired at 2100 cm^{-1} . Spurious background (e.g. from the surrounding media) is due to nonresonant four wave mixing. (e) Real-time background subtraction via FM-CARS leaves only the lipid droplets which have accumulated the deuterated fatty acids with visible contrast in the image. Scale bar: $10\text{ }\mu\text{m}$.

The FM technique can also be applied to mammalian cells to detect a small amount of deuterium. Human lung cancer (A549) cells were grown with 3 mM deuterated oleic acid in the culture medium for two hours. The cells were then fixed and imaged with normal CARS

and FM-CARS. In the normal CARS image (Fig. 4d), the nonresonant background yields spurious contrast that is not due to the chemical features of the sample (e.g. from the surrounding media despite the fact it was washed to remove deuterium). In contrast, in the FM-CARS image (Fig. 4e), only lipid droplets that have accumulated the deuterium from the fatty acids appear. This is not equivalent to simply subtracting a constant background from the image in Fig. 4d, because the nonresonant background varies spatially.

An additional possibility is to use this OPO to implement a frequency modulation detection scheme for SRS. In our previous implementation of SRS, one beam (e.g. the pump beam) was amplitude modulated [6], and the modulation transferred to the other beam via the stimulated Raman scattering process was detected. Here, we replace the amplitude modulation with frequency modulation. For SRS imaging, we modified our microscope by adding a higher NA condenser (0.8 NA air) and replacing the PMT detector with a photodiode (FGA21, Thorlabs). The pump beam was blocked with a filter that transmitted only the Stokes wavelength (D1125/150m, Chroma Technology), and stimulated Raman gain (SRG) of the Stokes beam was detected by modulating the pump wavelength on and off resonance as in FM-CARS.

Figure 5a shows the SRG image of minoxidil-d10 (CDN Isotopes) on the surface of wild-type white mouse skin. Minoxidil is a skin-active compound used for promoting hair regrowth and in this case was obtained from a commercial supplier with a deuterium label to provide a unique vibrational signature. Tuning the laser to match the C-²H resonance as above, we were able to visualize the distribution of the drug on the surface (Fig. 5a). In the normal epi-CARS image (Fig. 5b), nonresonant features such as the mouse hair appear with almost equal intensity to the drug, again making identification of the chemically specific information difficult. This is manifestly true even on a qualitative level, i.e. whether or not the drug accumulates in hair cannot be distinguished because of the background signal in CARS, while the frequency modulation SRG channel shows that it does not.

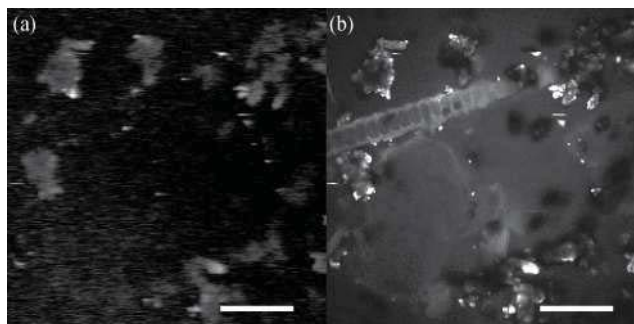


Fig. 5. (a) A frequency modulation SRG image of the surface of mouse skin shows the accumulation of the minoxidil-d10 on the surface, and is free of the nonresonant background that troubles CARS. In this case, no amplitude modulation was necessary to detect the signal. (b) Normal CARS image of the same area as (a). In normal CARS, the strong nonresonant background from the hair makes distinguishing chemical from structural features impossible, even on a qualitative level. Scale bar: 50 μ m.

4. Summary

We have described a novel picosecond optical parametric oscillator which provides rapid frequency modulation and operating characteristics (pulse width, wavelength, repetition rate) that are well suited for CRM. We have demonstrated that this source can be used to perform chemically selective imaging using the FM-CARS and frequency modulation SRS imaging modalities. The modulation frequency, 38 MHz, is the highest possible to achieve with a 76 MHz pump laser, and with faster demodulation circuitry could allow measurement times approaching 26 ns.

Because SRS is free of the nonresonant electronic background, future applications of this device would likely be based on that technique rather than FM-CARS. Compared to the previous amplitude modulation approach for SRS detection [6], a frequency modulation approach would reduce the spurious background from two-color two-photon absorption, thermal lensing and cross phase modulation. While cross-phase-modulation and thermal lensing can be reduced by using a high numerical aperture condenser for light collection [5], SRS and two-color two-photon absorption are optically undistinguishable and thus are best distinguished based on the spectral response. In addition, under non-ideal collection conditions (e.g. when using an optical fiber with low numerical aperture for collection), cross-phase-modulation is expected to make SRS detection by amplitude modulation problematic. A frequency modulation approach would be beneficial in those cases as well.

Further applications of the double-cavity-length scheme described here will likely be found where rapid wavelength modulation of an ultrafast pulsed light source such as an optical parametric oscillator or a titanium:sapphire laser, is desirable.

Acknowledgments

We thank J. MacArthur for invaluable support on the drive electronics, H. Chen for preparing the deuterated samples, and C. L. Evans for helpful discussions. B.G.S was supported by the Army Research Office through an NDSEG Fellowship. C.W.F. was supported by a Boehringer Ingelheim Fonds Ph.D. Fellowship. Support for this work was provided by the U. S. National Science Foundation (grant DBI-0649892) and the U. S. Department of Energy (grant DE-FG02-07ER64500).